IJISEM
INTERNATIONAL JOURNAL OF INNOVATIONS IN SCIENCE ENGINEERING AND MANAGEMENT

Examine the Heat Transfer Characteristics in Car Radiator Utilizing the Water/Anti-Freezing and Al_2O_3/Cuo/Tio_2 Based Nanofluid as Coolant

Rohit Khare[1], Dr. Dharmendra Tyagi[2]

[1]*Research Scholar, Dept. of Mechanical Engineering, Sagar Institute of Research and Technology*
[2]*Associate Professor, Dept. of Mechanical Engineering, Sagar Institute of Research and Technology*

OPEN ACCESS

Volume: 4

Issue: 1

Month: January

Year: 2025

ISSN: 2583-7117

Published: 07-01.2025

Citation:

Rohit Khare, Dharmendra Tyagi, 'Examine the Heat Transfer Characteristics in Car Radiator Utilizing the Water/Anti-Freezing and Al_2O_3/Cuo/Tio_2 Based Nanofluid as Coolant, International Journal of Innovations In Science Engineering And Management, vol. 4, no. 1, 2025, pp.17-30

DOI

10.69968/ijisem.2025v4i117-30

Abstract

Automobile radiators have been using traditional heat transfer fluids like water and motor oil for a long time. However, there is an increasing demand for improved heat transfer fluids in order to greatly increase the system's thermal performance. Traditional fluids often suffer from low thermal conductivities, and the flat tube's limited surface area hinders the enhancement of heat transfer. Improving heat transmission between the radiator and coolant is primarily intended to increase the cooling capability of car engines, guaranteeing peak performance and averting malfunctions. This study investigates two methods to achieve this goal. The first method focuses on modifying the radiator's flat tube design by altering the fin configuration. One design incorporates 34 continuous louvered fins, while the other uses 46 continuous louvered fins with a U-shaped configuration. In order to improve heat transmission, the second technique adds solid particles that are nanoscale in size to the base fluid. Three nanoparticles—Al_2O_3, CuO, and TiO_2—are used at concentrations of 0.05%, 0.15%, and 0.3%. By combining these modified designs with various nanoparticle concentrations, a total of 10 cases were analyzed. Throughout the investigation, the flat tube's coolant's intake velocity remained constant. ANSYS Fluent 23.2 was used to assess the heat transfer properties, taking into account variables including velocity distribution, temperature distribution, pressure drop, and heat transfer rate. The coolant containing 0.3% TiO_2 nanoparticles had the greatest heat transfer capability, surpassing all other examples examined. Its outlet temperature was 360.53 K, and its heat transfer rate was 76.73 W.Keyword: Diabetes detection, machine learning, Support Vector Machine, Gradient Boosting, voting ensemble, early diagnosis.

Keywords: Nanopaticles, Radiator, heat transfer, Ethylene glycol, Louvered fins, etc.

I. INTRODUCTION

A. Background

The issue of inadequate heat dissipation rates in automobile radiators has come up as a result of the need for more potent engines in smaller hood areas. Up to 33 percent of the engine's combustion-based energy is wasted as heat [1]. An engine that overheats due to inadequate heat dissipation may break down its lubricating fluid, damage its metal components, and experience considerable wear between them [2]. Reducing the load that heat generation puts on the engine requires that automotive radiators be made smaller while maintaining strong heat transfer performance. The engine of a vehicle produces power via the combustion of petrol and air. The majority of the power generated is wasted as heat and exhaust, with just a tiny portion actually being utilised to drive the vehicle [3], [4]. Failure to remove this excess heat results in an excessively high engine temperature, which increases wear on the related moving posts by causing lubricating fluid viscosity failure, excessive heat, metal degradation of the overheated components of the engine, and stress between engine parts. A cooling system takes away the extra heat [5]. Most automobile cooling systems consist of a "water pump, radiator, electric cooling fan, thermostat, and radiator pressure cap". The most obvious part of the

system is the radiator, which transfers heat. As coolant flows across the engine's cylinder block, heat is generated [6]. When the car's coolant temperature reaches a specific degree, the thermostat opens a valve that forces the coolant to pass through the radiator. Using both the tube and fin walls, the coolant travels via the radiator's tubes, transferring heat to the air by convection and conduction [7], [8].

Internal combustion engines, that are mostly used in automobiles but are also present in piston-engine aircraft, railroad locomotives, motorcycles, stationary power plants, and other similar equipment, are cooled by heat exchangers known as radiators [9]. A liquid known as engine coolant is often circulated through the engine block and cylinder head to heat the engine, then via a radiator to release the heat into the environment before being recirculated back into the engine to cool internal combustion engines [10]. Although it may also be oil-based, engine coolant is mostly water-based. Air is typically forced into the radiator by an axial fan, and the engine coolant is urged to circulate by a water pump. Aluminium radiators are seen in most contemporary automobiles. Thin aluminium fins are brazed on flattened aluminium tubes to create these radiators [11]. From the entry to the exit, the coolant is transported by many tubes that are positioned in parallel. The air moving through the radiator receives heat from the tubes via the fins. To increase the turbulent flow of the fluid moving through the tubes, a fin called a turbulator has been inserted [12].

A vehicle engine must be continuously cooled to avoid damage since it produces a lot of heat while running. This is usually done by circulating coolant liquid, which is usually water mixed with an antifreeze solution, via dedicated cooling tubes [13]. Coolant channels join the cylinder head and engine block of a water-cooled engine. At the peak of the cylinder head, nearly all the channels combine to create a single outlet [14]. A crankshaft pulley-and-belt-powered pump transfers hot coolant coming from the engine to the radiator, acting as a kind of heat exchanger. Through an inlet at the bottom of the block, the cooled liquid returns to the channels after the radiator has transferred surplus heat towards the air stream [13]. The pump usually moves coolant up by the engine and decreases via the radiator because heated hot water expands, becomes thinner, and increases above cold water. The pump aids in circulation, and it naturally tends to flow upward [15]. The radiator is connected to the engine via rubber hoses, and the top and bottom tanks are connected by a core, which is a bank of numerous small tubes. The tubes flow through nine openings in an arrangement of "thin sheet-metal fins" to provide the core a large surface area and have the capacity to rapidly transfer heat to the cooler air passing past it [16]. Modern, low-fronted automobiles feature crossflow radiators with side-to-side tubes, whereas older cars have vertical tubes. An engine's coolant is only a little bit below the boiling point at normal operating temperatures. Boiling is less likely as the system's pressure is increased, which raises the boiling point [17]. The extra pressure is limited by the radiator cap's pressure valve. An overflow pipe allows coolant to escape when excessive pressure opens the valve. A little quantity of coolant is continually lost in such a type of cooling system if the engine runs too hot [18]. The system must be topped up on a regular basis. Later versions have a sealed system, which directs any overflow towards an expansion tank before being pulled away from the engine after the remaining liquid has cooled [19].

II. OBJECTIVE

- Using the CFD approach, numerically examine the radiator's performance using water, ethylene glycol as the base fluid, and nanoparticles as the working fluids (coolant).
- Investigate the radiator performance with various concentration of nanoparticle.
- Investigate the effect of variation in number of fins in performance of radiator.
- Investigate the heat transfer rate in radiator using various nanofluid.
- Investigate the temperature, pressure and velocity behavior of the coolant (fluid) in radiator.

III. METHODOLOGY

A. Governing equation

The fluid flow within the flat tube is controlled using the following formulas.

Steady-state continuity equation:

$$\frac{\partial}{\partial x_i}(\rho u_i) = 0$$

Incompressible and time-independent The Navier-Stokes equation:

$$\frac{\partial}{\partial x_i}(\rho u_i u_j) = -\frac{\partial P}{\partial x_i} + \frac{\partial}{\partial x_j}\left[\mu \frac{\partial u_i}{\partial x_j} + \frac{\partial u_j}{\partial x_i}\right] + \frac{\partial}{\partial x_i}(-\rho \acute{u}_i \acute{u}_j)$$

In the direction of xi, i≠j, P, ρ, μ, ui, and u′i stand for pressure, fluid density, dynamic viscosity, and the mean and changeable components of velocity, respectively.

Energy formula

$$\rho c_p u_i \frac{\partial T}{\partial x_i} = \frac{\partial}{\partial x_j}\left[\left(\mathscr{T} + \mathscr{T}_t\right)\frac{\partial T}{\partial x_j}\right]$$

The thermal diffusivity of thermal and molecular thermal diffusivity are denoted by $\mathscr{T}$and $\mathscr{T}_t$, respectively.

Using steady-state transport equations, the standard $K-\varepsilon$ turbulence model is used as:

$$\frac{\partial}{\partial x_j}(\rho\varepsilon u_i) = \frac{\partial}{\partial x_i}\left(\alpha_\varepsilon \mu_e \frac{\partial \varepsilon}{\partial x_i}\right) + C_1\frac{\varepsilon}{k}G_k - C_2\rho\frac{\varepsilon^2}{k}$$

$$\frac{\partial}{\partial x_j}(\rho k u_i) = \frac{\partial}{\partial x_i}\left(\alpha_k \mu_e \frac{\partial k}{\partial x_i}\right) + G_k - \rho\varepsilon$$

$$\mu_e = \mu + \rho C_u \frac{k^2}{\varepsilon}$$

The turbulent kinetic energy is denoted by K, the rate of dissipation by˘, and the effective viscosity by μe. We have defined k, ε, and μe using Eqs. 4, 5, and 6, respectively. where the values of the variables α˘, αk, C_1, C_2, and Cu are 1.39, 1.39, 1.44, 1.92, and 0.0845, respectively.

B. Model equations of the nanofluid physical properties

The following mathematical models were first used to ascertain the basefluid and nanofluid's thermo-physical characteristics. ANSYS Fluent software was used to do the computed fluid dynamics analysis using these characteristics. The basic fluid, which is ethylene glycol and water, was combined with the nanoparticles. It was believed that the nanoparticles were consistent across the system and evenly distributed throughout the mixture. Several formulae have been used by different researchers throughout the years to ascertain the thermo-physical characteristics of nanofluids. Utilising the following formulas, the nanofluid's "density, specific heat capacity, and thermal conductivity" were determined:

$$\rho_{nf} = \varphi\rho_p + (1-\varphi)\rho_{bf} \qquad 1$$

$$\left(\rho C_p\right)_{nf} = \left(\rho C_p\right)_p + (1-\varphi)\left(\rho C_p\right)_{bf} \qquad 2$$

$$k_{nf} = \frac{k_p + (\Phi-1)k_{bf} - \varphi(\Phi-1)\left(k_{bf}-k_p\right)}{k_p + (\Phi-1)k_{bf} + \varphi\left(k_{bf}-k_p\right)}k_{bf} \qquad 3$$

The empirical shape factor, Φ, is determined by the formula Φ=3⁄ψ. The particle sphericity, or ψ, is the ratio of the particle's surface area to "the surface area of a sphere" having a volume equal to the particle's. A common assumption in numerous literatures is that the nanoparticle in this work is a perfect sphere with a sphericity of ψ=1. "The empirical shape factor Φ=3" is estimated with the support of this assumption. The viscosity of ethylene glycol-based and mixture-based nanofluids has been ascertained using this correlation:

$$\mu_{nf} = \mu_{bf} + \frac{\rho_p V_B d_p^2}{72C\delta} \qquad 4$$

where the fluid's apparent viscosity, which results from the impact of nanoparticles, is the second term. The following formula is used to get the distance (d) between the nanoparticle centres and the correction factor (C):

$$\delta + \sqrt[3]{\frac{\pi}{6\varphi}}d_p \qquad 5$$

$$C = \frac{a\varphi+b}{\mu_{bf}} \qquad 6$$

where a and b stand for experimental parameters, which were calculated to be "0.00004 and 7.1274 × 10-7", respectively, for the engine coolant nanofluids.

In this work, utilize three nanoparticle for improving the coolant thermo-physical properties. In radiator flat tubes, a combination of "water and ethylene glycol" was used as the base fluid, also referred to as coolant flow. Table 1 displays the thermo-physical characteristics of the base fluid, which is a combination of ethylene and water. The three nanoparticles used in the research are "aluminium oxide (Al_2O_3), copper oxide (CuO), and titanium dioxide (TiO_2)". Table 1 lists the thermo-physical characteristics of each. Volume concentration of 0.05, 0.15, and 0.3% of each nanoparticle are mixing with base fluid. Table 2 lists the thermo-physical characteristics of the base fluid augmented nanofluid.

C. Rate of heat transfer

The Nusselt number, heat transfer coefficient, rate of heat transfer, and thermal conductivity were used to measure the heat transfer parameters. Using the mathematical model, the nanofluids' Q, or rate of heat transmission, was determined as follows:

$$\dot{Q} = \dot{m}C_p(T_{inlet} - T_{outlet}) \qquad 7$$

Table 1 Thermo-physical properties of base fluid and nanoparticle [20][21]

Specification	Units	Base fluid (Water + EG)	Aluminium oxide (Al2O3)	Copper oxide (CuO)	Titanium dioxide (TiO2)
Grain size	(nm)	-	20	60	21
Purity	(%)	-	+99	+98	99.5
Specific heat	(J/kg K)	3570	765	535.6	686.2
Density	(kg/m3)	1027.01	3970	6500	4250
Thermal conductivity	(W/m K)	0.415	46	20	8.9
Viscosity	(kg/m s)	0.00076	-	-	-

Table 2 Thermo-physical properties of base fluid enhance nanofluid [20]

Volume concentration	Properties			
	Density (kg/m3)	Specific heat capacity (J/kg K)	Thermal conductivity (W/m K)	Viscosity (kg/m s)
	Water + Ethylene Glycol (EG) + Al_2O_3			
0.05	1156.10	3461.123	0.668	0.0019
0.15	1452.3	2685.322	0.874	0.0019
0.3	1896.6	1975.971	1.287	0.0019
	Water + Ethylene Glycol (EG) + CuO			
0.05	1282.6	3137.082	0.664	0.0019
0.15	1831.8	2165.382	0.858	0.0019
0.3	2655.6	1461.414	1.241	0.0019
	Water + Ethylene Glycol (EG) +TiO_2			
0.05	1188.16	3054.24	0.472	0.00143
0.15	1510.46	2352.87	0.565	0.0052
0.3	1993.907	1725.96	0.856	0.0365

D. Geometry description

Based on the design data gathered from other publications, the automobile radiator model was created in CATIA software and then loaded into ANSYS Fluent software. Flat tubes with louvred and U-shaped fins made up the automobile radiator. Additionally, the radiator's aluminium material was incorporated into the design. The ANSYS program has limits, thus only a section of the fins and flat tube were imported for further analysis. Figure 1 provides detailed demonstrations of the flat tube's geometrical configurations. The geometrical parameter of the vehicle radiators employed in this investigation are shown in the table 3. In this work two design of radiator consider, while the changes happen in fins patterns. The radiator design consist of 34 fins having continuous louvered fin show in figure 2(a) and radiator design consist of 46 fins having continuous louvered fin and "U-shape" fins show in figure 2(b). In both design of radiator no changes make on geometry of flat tube. The following is how the mathematical model was used to determine the flat tube's hydraulic diameter:

$$d = \frac{2ab}{a+b} \qquad 8$$

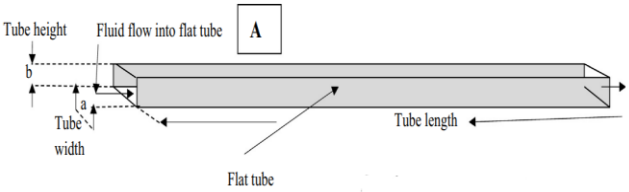

Figure 1 Geometrical parameter notation representation of flat tube

Table 3 Automobile radiator model's geometrical parameter.

Parameter	Unit	Value
Tube thickness	cm	0.5
Tube length	cm	31.5
Tube width	cm	2
Tube height	cm	0.3
Fin height (Louvered shape)	cm	1.25
Number of fins	-	34, 46
Space between tubes	cm	1.5
Fin height (U-shape)	cm	0.7
Material used	-	Aluminium
Tube hydraulic diameter	cm	0.52

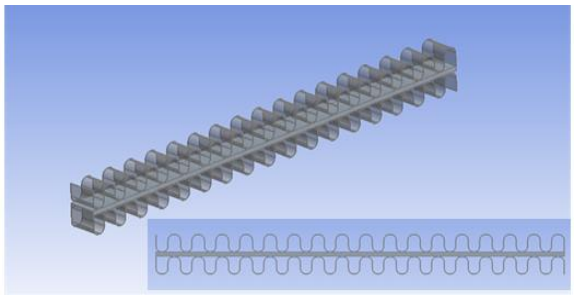

(a) Radiator design having (34 fins)

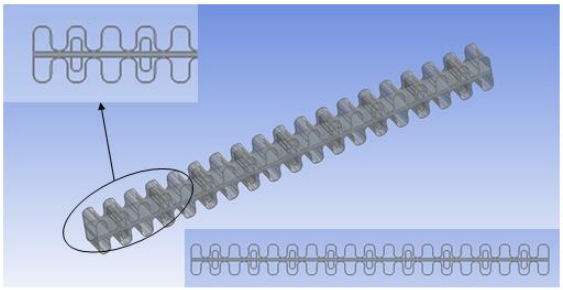

(b) Radiator design having (46 fins)

Figure 2 Geometry description of radiator design

E. Mesh generation

Due to its direct impact on the convergence and correctness of the findings, mesh creation is an essential stage in numerically simulating coolant in flat tube of radiator. The computational domain in this work was discretized using “hexahedral and tetrahedral mesh” components. Tetrahedral mesh select of tube, fins domain, and hexahedral mesh select for coolant domain. The mesh element count and corresponding nodes for each design are summarized in a tabular format. Mesh element size is 0.002 m were applied. This approach allowed for efficient refinement of critical regions while maintaining computational feasibility. The combination of tetrahedral and hexahedral mesh elements provided flexibility in handling irregular geometries and ensured accurate resolution of flow and thermal gradients within the duct.

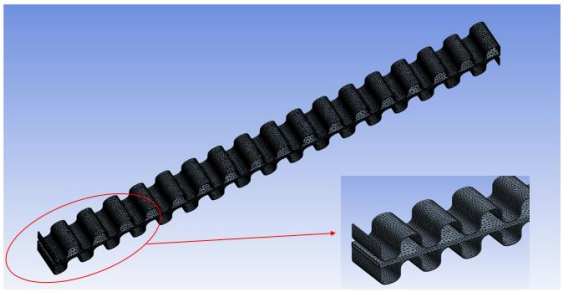

Figure 3 Generated mesh in radiator having 34 fins

F. Boundary condition

The "ANSYS FLUENT version 23" was used to simulate the radiator. Important factors, such as wall conditions, pressure outlet, intake velocity, and inlet temperature, were carefully subjected to boundary conditions. A constant intake temperature of 95°C (368.15 K) was maintained, and the coolant inlet velocity was set at 0.077 m/s, giving a "volumetric flow rate of 6 L/min". The flat tube's hydraulic diameter, which reflected the radiator tube's proportions, was initially set at 0.0052 m. The flat tube wall was modelled using a convection boundary circumstance, with the temperature of the surrounding air taken to be 35°C and "the heat transfer coefficient" set at 10 $W/m^2 \cdot K$.

For turbulence modeling, the k-epsilon model was employed due to its robustness in simulating turbulent flows. For pressure-velocity coupling, the SIMPLE scheme was used, and for the spatial discretisation of "pressure, momentum, and energy", a second-order upwind scheme was used. The "pressure, momentum, and energy" under-relaxation factors were set at 0.3, 0.7, and 1.0, respectively, to guarantee solution stability. The radiator design consisted of two configurations: one with 34 continuous louvered fins and another with 46 fins, which included U-shaped fins added alternately for enhanced performance. However, for computational feasibility, only a single flat tube and its associated fins were simulated in ANSYS FLUENT. Several assumptions were made to simplify the simulation and numerical calculations. It was assumed that the flow within the radiator was steady, incompressible, and turbulent. Throughout the flow, the coolant's thermophysical characteristics were also thought to remain constant. These assumptions allowed for a more manageable simulation process while maintaining sufficient accuracy to evaluate the radiator’s performance.

Using the three nanoparticle (Al_2O_3, CuO, and TiO_2) with concentration of 0.05, 0.15, 0.3% mixing with base fluid as a coolant introduce various scenarios which is consider for evaluate the performance of radiator. The various scenarios are mention in the table 6. Further design and performance optimisation of the radiator is made possible by this thorough simulation technique, which offers insightful information on the radiator's fluid and thermal flow properties.

Table 4 Mesh generation details

Design	No. of fins	Elements	Nodes
Design 1	34 Nos.	161240	57384
Design 2	46 Nos.	285638	98999

Table 5 Parameters for boundary condition

Parameter	Unit	Value
Coolant inlet temperature	°C (K)	95 (368.15)
Coolant inlet velocity	m/s (L/min)	0.077 (6)
Hydraulic diameter of flat tube	m	0.0052
Heat transfer coefficient of wall	W/m2K	10
Surrounding air temperature	°C (K)	35 (308.15)

Table 6 Case description

Case notation	Design of radiator	Base fluid	Nanoparticle	Concentration
Case 1	34 fins	Water + Ethylene Glycol (EG)	CuO	0.3
Case 2	46 fins		Al_2O_3	0.05
Case 3	46 fins		Al_2O_3	0.15
Case 4	46 fins		Al_2O_3	0.3
Case 5	46 fins		CuO	0.05
Case 6	46 fins		CuO	0.15
Case 7	46 fins		CuO	0.3
Case 8	46 fins		TiO_2	0.05
Case 9	46 fins		TiO_2	0.15
Case 10	46 fins		TiO_2	0.3

G. Validation

By contrasting the simulation results with the experimental findings, the validation procedure was carried out to guarantee the correctness of the simulation results (Tijani and Sudirman, 2018) [20]. This fluid was made out of a base fluid combination of ethylene glycol and water, with 0.3% volume concentration of CuO nanoparticles distributed throughout. The validation focused on comparing the outlet temperature of the coolant obtained from the simulation with the results reported by (Tijani and Sudirman, 2018) [20]. A mathematical methodology that guaranteed the simulation's correctness and dependability further reinforced this comparison. Figure 4 illustrates the temperature distribution along the radiator wall as obtained from both (Tijani and Sudirman, 2018)'s [20] results and the present simulation, demonstrating a close match in the thermal behavior. Additionally, Figure 5 shows a detailed comparison of the coolant's outlet temperature, validating the consistency between both simulated results. The validation process recorded an average error of 0.12%, which is considered negligible. As such, the simulation results are deemed validated and reliable for further analysis. This close agreement highlights the robustness of the computational model and its ability to accurately replicate the thermal and flow behavior observed in the experimental setup.

IV. RESULT AND DISCUSSION

This section examines the influence of various nanoparticles, at different concentrations, mixed with a base fluid used as coolant flowing inside the flat tube of the radiator. The study evaluates the performance of the flat tube and analyzes performance characteristics under various scenarios outlined in Table 6. "The rate of heat transfer" inside the flat tube, pressure change, velocity profiles, and temperature distribution are important performance factors.

This study aims to improve the radiator's overall efficiency by studying the effects of various nanoparticle kinds and concentrations on the base fluid's heat transmission capacities. Contour plots of temperature, velocity, and pressure distributions, along with the rate of heat transfer, provide visual insights into the flow and thermal performance for each scenario. These results are critical for identifying the optimal nanoparticle concentration and type for achieving maximum heat dissipation and ensuring the efficient operation of the radiator.

By analyzing these performance characteristics, this study contributes to understanding the impact of nanofluids on radiator performance, paving the way for advanced coolant designs tailored to specific thermal management requirements.

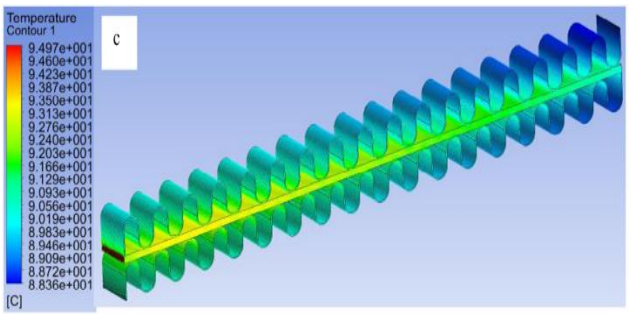

(a) (Tijani & Sudirman, 2018)[20]

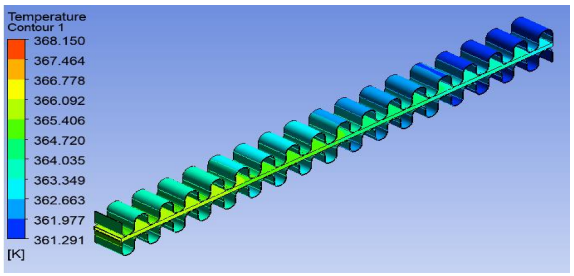

(b) Present simulation

Figure 4 Temperature contour validate with CuO nanoparticle at 0.3% volume concentration

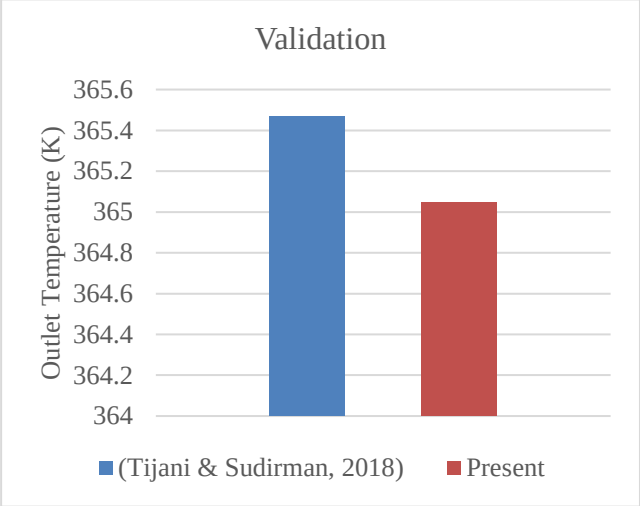

Figure 5 Outlet temperature result validate of radiator

A. Performance characteristics in 36 fins flat tube

Figure 6(a) shows the distribution of temperatures inside the radiator's tube body, whereas Figure 6(b) shows the same data for the coolant. The temperature distribution is represented by a color gradient, ranging from the minimum to the maximum temperature achieved in Case 1. The temperature of the surrounding air is 308.15 K, and the coolant temperature is 368.15 K as it enters the flat tube. Because of convection, heat moves from the coolant into the tube, where it is dissipated at a rate of 10 W/m²·K by the surface of the tube. A mechanism known as convection controls the passage of heat from the cooler's higher temperature to the tube's lower surface temperature. The figures illustrate that as the coolant flows through the flat tube, its temperature gradually decreases, while the temperature of the tube increases. The maximum temperature, observed at the coolant inlet, is 368.15 K, while the minimum temperature is 361.29 K in the tube and approximately 365.4 K in the coolant. These differences demonstrate how well the coolant transfers heat to the tube body.

The coolant flow velocity distribution within the flat tube is seen in Figure 7. The coolant enters at an initial velocity of 0.077 m/s, and the maximum velocity, 0.082 m/s, is observed in the central region of the coolant flow. Near the tube walls, the velocity decreases due to the no-slip condition, resulting in a laminar flow region.

Figure 8 illustrates the pressure distribution within the coolant as it flows through the flat tube. At the inlet, the pressure is at its maximum, recorded as 50.878 Pa, and it decreases progressively as the coolant travels along the tube. The relationship between pressure and temperature is evident; higher pressure is observed at regions with higher temperatures. At the outlet, the pressure reaches its minimum value of 0 Pa, corresponding to the lower temperature at this point. This steady drop in temperature and pressure throughout the flow channel is a result of both fluid dynamics and heat transfer in the radiator. Together, these numbers help to understand the radiator's performance and efficiency by shedding light on the fluid flow and thermal behaviour of the coolant.

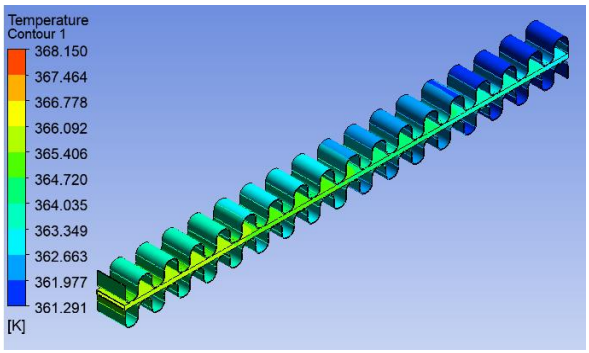

(a) In flat tube with fins

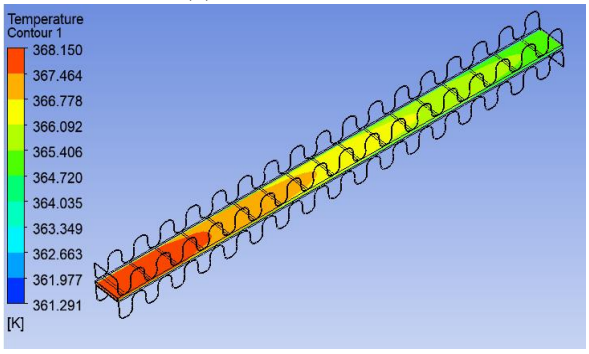

(b) In coolant

Figure 6 Temperature distribution in case 1

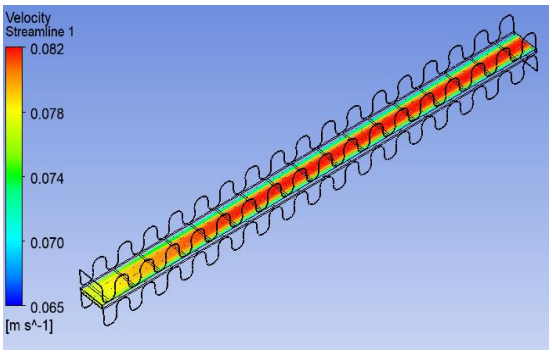

Figure 7 Velocity distribution in case 1

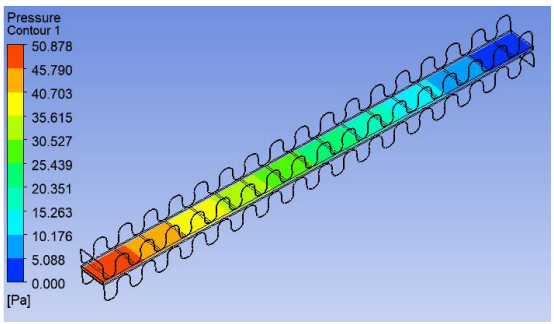

Figure 8 Pressure distribution in case 1

B. Temperature distribution in 46 fins flat tube

For each of the scenarios under consideration, the temperature distribution in the radiator's flat tube and coolant is shown in Figures 9 and 10, respectively. The temperature variation is illustrated using a color gradient, which ranges from the minimum to the maximum temperature achieved in each individual case. The maximum temperature in all cases stays at 368.15 K, which is the system's highest temperature and corresponds to the coolant intake temperature. Heat transfer occurs via convection, where thermal energy flows from regions of higher temperature (coolant) to lower temperature (flat tube). Because of this, the coolant's temperature reaches its maximum at the intake and gradually drops as it moves along the tube. Both the flat tube and coolant temperature distributions are depicted in the figures.

When Al_2O_3 nanoparticles are used at concentrations of 0.05%, 0.15%, and 0.3% (corresponding to cases 2, 3, and 4), the minimum temperature in the flat tube at the outlet is observed to increase with nanoparticle concentration. Specifically, the minimum temperatures are 356.179 K, 357.489 K, and 358.546 K for cases 2, 3, and 4, respectively. Similarly, in the coolant at the exit, the minimum temperatures are approximately 361.88 K, 361.84 K, and 361.838 K for the same cases. As shown by the slow increase in the flat tube's minimum temperature and the minor decrease in the coolant's exit temperature, these findings suggest that increasing the concentration of Al_2O_3 nanoparticles enhances heat transmission.

A similar pattern is shown for CuO nanoparticles at percentages of "0.05%, 0.15%, and 0.3% (cases 5, 6, and 7)". The minimum temperatures in the flat tube are 356.44 K, 357.738 K, and 358.467 K for cases 5, 6, and 7, respectively. As the percentage of CuO nanoparticles rises, the tube and coolant temperatures rise as well. The exit minimum temperatures in the coolant are around "361.755 K, 361.982 K, and 361.916 K". This enhancement demonstrates how the coolant with larger nanoparticle concentrations performs better thermally.

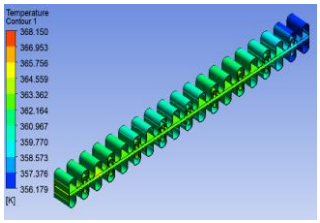

Case 2

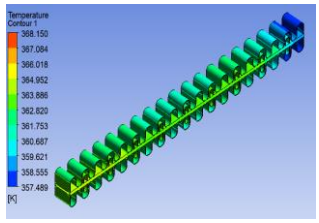

Case 3

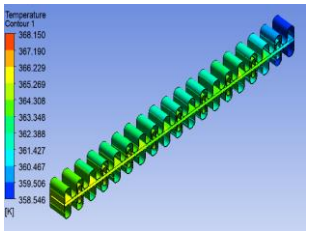

Case 4

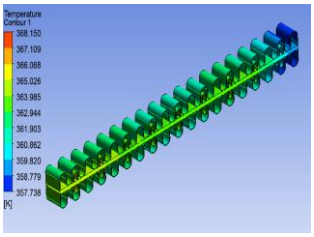

Case 5

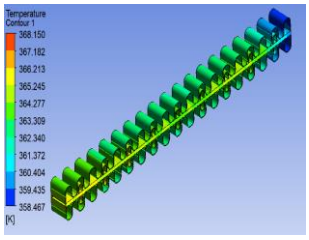

Case 6

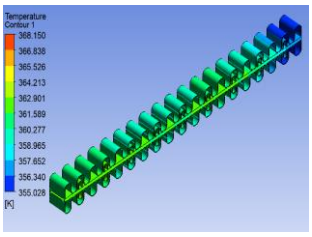

Case 7

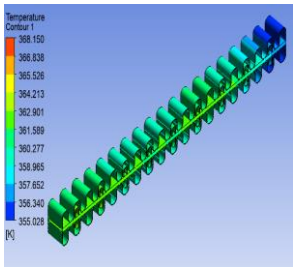

Case 8

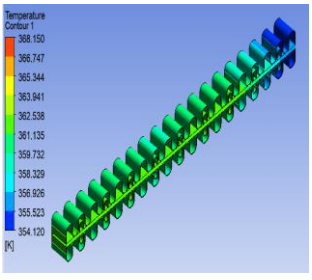

Case 9

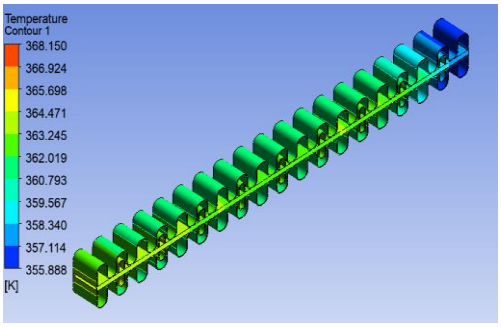

Case 10

Figure 9 Temperature distribution at flat tube in case 2-10

In the case of TiO_2 nanoparticles at concentrations of 0.05%, 0.15%, and 0.3% (cases 8, 9, and 10), the minimum temperatures in the flat tube at the outlet are 355.028 K, 354.120 K, and 354.888 K, respectively. The minimum temperatures in the coolant at the exit are approximately 361.412 K, 360.78 K, and 360.53 K. These results show that while the flat tube temperature increases with higher TiO_2 concentrations, the coolant temperature at the exit decreases, reflecting the improved heat dissipation achieved with TiO_2 nanoparticles.

Overall, increasing the concentration of nanoparticles, regardless of type, leads to better thermal performance by enhancing heat transfer. This is evident from the temperature trends in both the flat tube and the coolant across all cases.

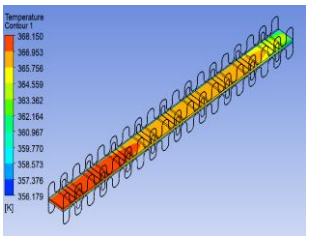

Case 2

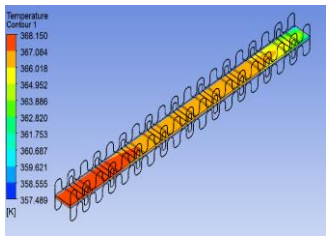

Case3

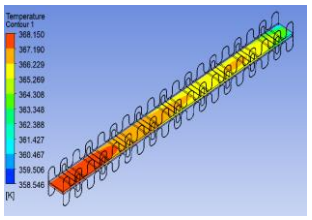

Case 4

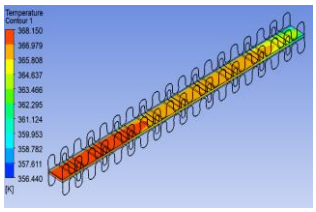

Case 5

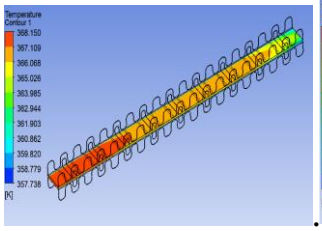

Case 6

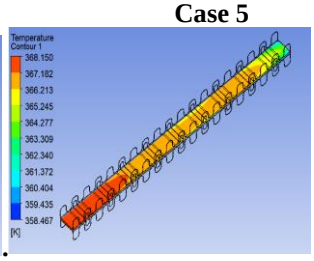

Case 7

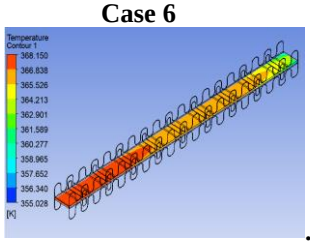

Case 8

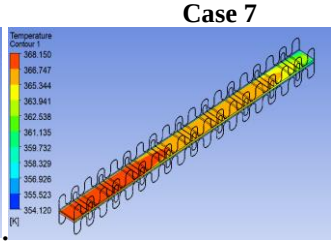

Case 9

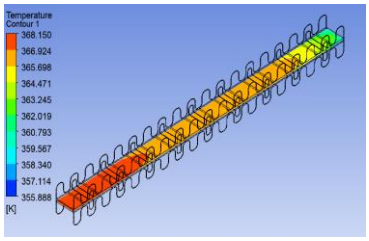

Case10

Figure 10 Temperature distribution at coolant domain in case 2-10

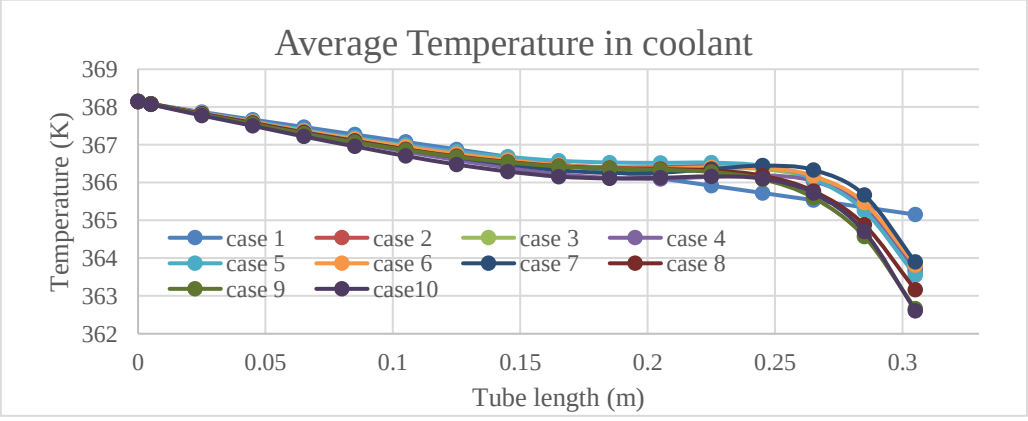

Figure 11 Average temperature in coolant along the tube length of case 2-case 10

Figure 13 illustrates a graphical comparison between the all cases from each nanoparticle—Al_2O_3, CuO, and TiO_2—in terms of their outlet temperatures and flat tube. Specifically, case 4, case 5, and case 10 represent the optimal scenarios for Al_2O_3, CuO, and TiO_2 nanoparticles, respectively, as they exhibit the lowest outlet temperatures among the tested cases for their respective nanoparticles. These cases utilize a flat tube design with 46 fins, which enhances heat transfer performance.

In contrast, case 1, which serves as the baseline, employs a flat tube design with 36 fins. The comparison between the effective cases (cases 4, 5, and 10) and the baseline case (case 1) highlights the influence of nanoparticle type and fin configuration on thermal performance. Among the effective cases, case 10, which involves TiO_2 nanoparticles, achieves the lowest outlet temperature. This indicates that the combination of TiO_2 nanoparticles at their optimal concentration and a flat tube with 46 fins delivers the most efficient cooling performance compared to other scenarios and the baseline case. Overall, the comparison underscores the significant role of both nanoparticle selection and radiator design modifications, such as increasing the number of fins, in achieving enhanced thermal performance.

C. Pressure distribution in 46 fins flat tube

Figures 12 illustrate the pressure distribution in the radiator's coolant for all considered scenarios. The pressure distribution is represented by a color gradient that varies from minimum to maximum pressure achieved within each case, particularly at the inlet and outlet of the flat tube. The highest pressure is observed at the inlet section, which differs across the cases, while the lowest pressure is consistently zero at the outlet section for all cases. This trend aligns with the relationship between temperature and pressure in the coolant, where pressure is directly proportional to temperature. At the inlet, where the temperature is at its peak, the pressure is also at its highest. As the coolant travels through the flat tube, both temperature and pressure gradually decrease due to heat transfer and flow dynamics.

For scenarios involving Al_2O_3 nanoparticles at concentrations of 0.05%, 0.15%, and 0.3%, corresponding to "case 2, case 3, and case 4", the maximum pressures recorded are 50.413 Pa, 50.482 Pa, and 50.553 Pa, respectively. The maximum pressure rises in proportion to the concentration of Al_2O_3 nanoparticles, which affects the properties of heat transmission and flow. Similarly, for CuO nanoparticles at the same concentrations, corresponding to "case 5, case 6, and case 7", the maximum pressures are observed to be 50.451 Pa, 50.543 Pa, and 50.651 Pa, respectively. As with Al_2O_3, the maximum pressure increases with the concentration of CuO nanoparticles. For TiO_2 nanoparticles, the pressure distribution exhibits a different pattern. At concentrations of 0.05%, 0.15%, and 0.3%, corresponding to case 8, case 9, and case 10, the maximum pressures recorded are 38.01 Pa, 137.6 Pa, and 961.477 Pa, respectively. Notably, the increase in pressure is more pronounced with higher concentrations of TiO_2 nanoparticles, reflecting their significant impact on flow resistance and heat transfer dynamics within the flat tube.

All things considered, the findings show that raising the concentration of nanoparticles, irrespective of their kind, raises the highest Pressure at the intake. However, the degree of pressure increase varies depending on the nanoparticle type, with TiO_2 showing the most substantial impact. These findings highlight the complex interplay between nanoparticle concentration, flow dynamics, and thermal performance in the radiator's coolant.

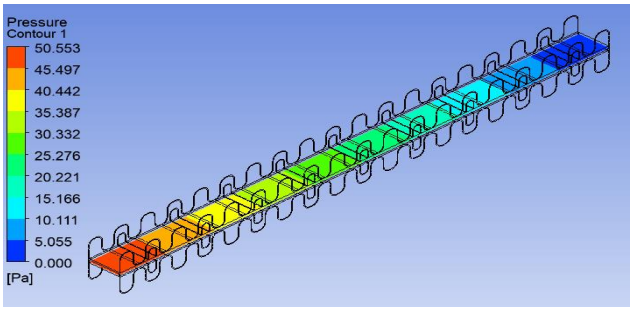

Case4

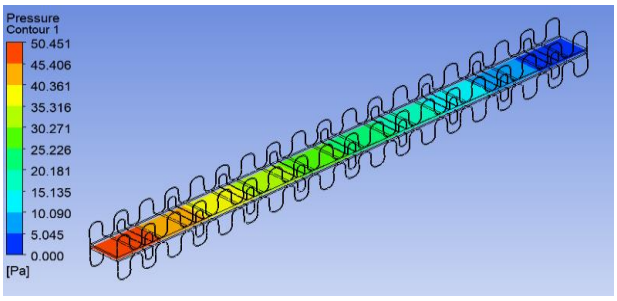

Case 5

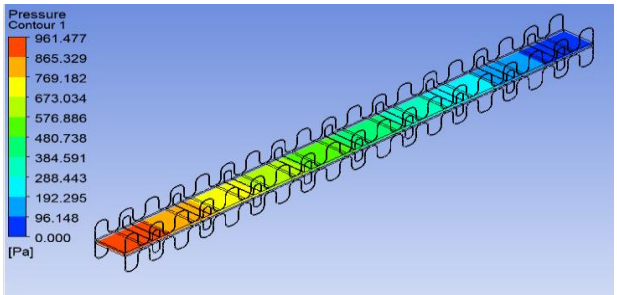

Case 10

Figure 12 Pressure distribution in effective cases

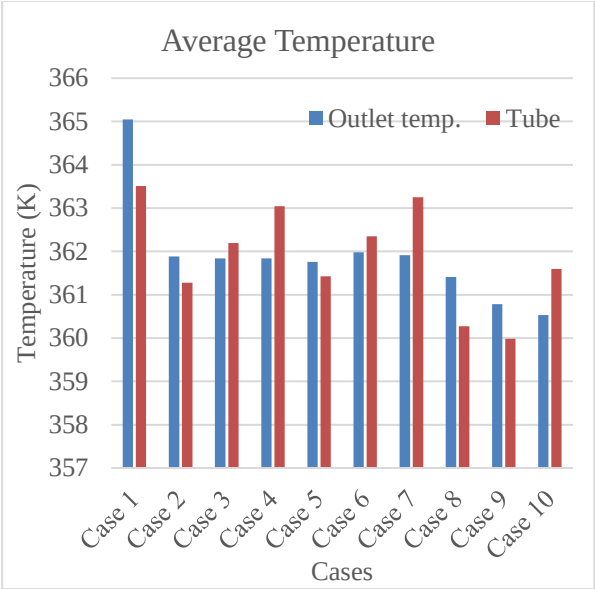

Figure 13 Average Temperature of tube and outlet coolant of case 2-case 10

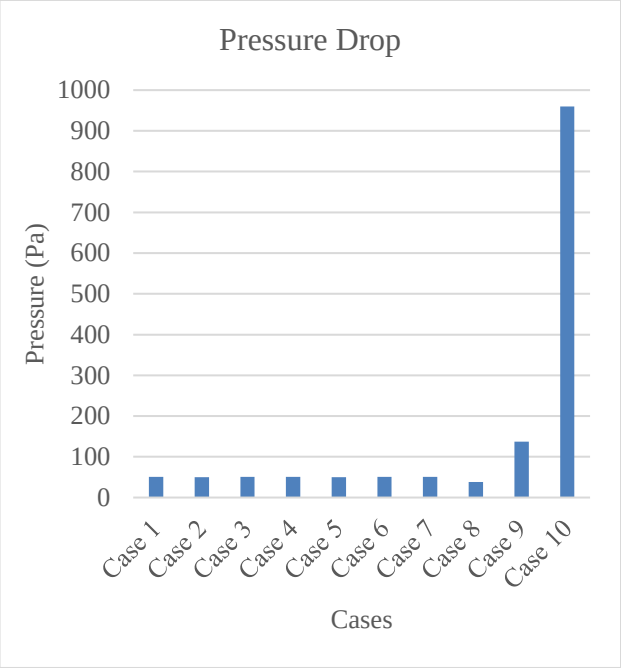

Figure 14 Pressure drop in case 2-10

D. Velocity distribution in 46 fins flat tubes

For every scenario taken into consideration, the coolant's velocity distribution as it flows within the flat tube is shown in Figures 15. The velocity distribution is depicted using a color gradient, representing variations from the minimum to maximum velocity achieved in each scenario. The coolant enters the flat tube with a velocity of 0.077 m/s at the intake, and the coolant flow's centre shows the highest velocity. Near the tube walls, the coolant flow stabilizes, indicating a region of minimal velocity due to boundary layer effects, where the flow is predominantly laminar.

For cases involving Al_2O_3 nanoparticles at concentrations of 0.05%, 0.15%, and 0.3%, corresponding to “case 2, case 3, and case 4”, respectively, the velocity distribution remains consistent with the expected flow dynamics. Similarly, for cases with CuO nanoparticles at the same concentrations, corresponding to “case 5, case 6, and case 7”, the distribution follows a comparable trend. Finally, for TiO_2 nanoparticles at concentrations of 0.05%, 0.15%, and 0.3%, corresponding to case 8, case 9, and case 10, the velocity profiles also align with the established pattern of fluid behavior in a flat tube.

Across all cases, the maximum velocity achieved is approximately 0.83 m/s, indicating that the nanoparticle type and concentration have minimal impact on the peak velocity within the coolant flow. The consistent maximum velocity across cases highlights the uniformity in flow behavior despite the variations in nanoparticle properties. This uniform velocity profile underscores the significance of nanoparticle concentration and type in influencing thermal performance while maintaining steady flow characteristics.

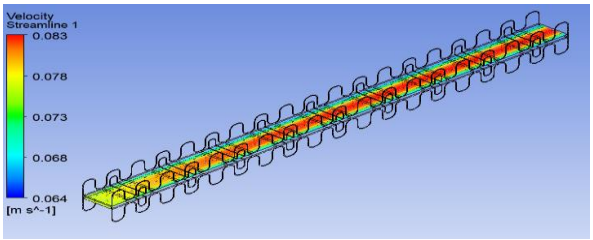

Case 4

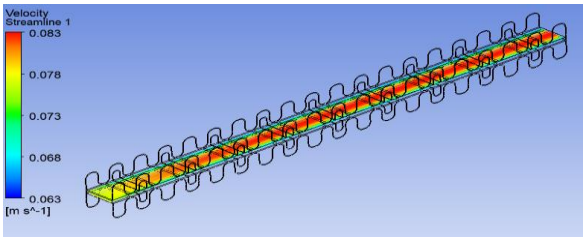

Case 5

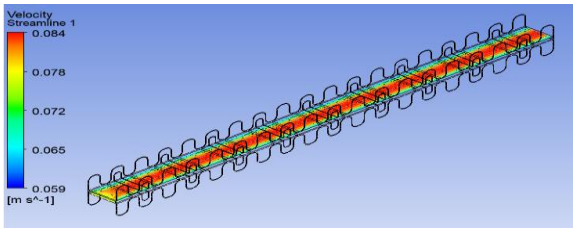

Case 10

Figure 15 Velocity distribution in effective cases

E. Rate of heat transfer

For each of the scenarios under consideration, Figure 16 shows "the rate of heat transfer (HT)" caused by convection among the coolant and the flat tube. In case 1, which involves a flat tube with 34 fins, the lowest heat transfer rate of 47.67 W is observed. The small surface area accessible for convection is the cause of this decreased heat transfer rate. Because the flat tube has 46 fins in “cases 2 to 10”, the additional surface area improves the rate of heat transmission.

For cases utilizing Al_2O_3 nanoparticles at concentrations of 0.05%, 0.15%, and 0.3% (corresponding to “case 2, case 3, and case 4”, respectively), the graph demonstrates a noticeable enhancement in heat transfer compared to case 1. Nevertheless, the rate of heat transmission somewhat drops when the concentration of Al2O3 nanoparticles rises. Case 2 shows best performance at the lowest concentration of nanoparticles for Al2O3, with an optimal "heat transfer rate of 73.37 W". The graph also shows a similar pattern for examples that use CuO nanoparticles at percentages of "0.05%, 0.15%, and 0.3%" (cases 5, 6, and 7, respectively). The heat transfer rate improves significantly compared to case 1, with the maximum value of 75.29 W recorded in case 5, where the CuO nanoparticle concentration is lowest. As the CuO nanoparticle concentration increases, a gradual decline in heat transfer efficiency is observed. In contrast, for cases utilizing TiO_2 nanoparticles at concentrations of 0.05%, 0.15%, and 0.3% (corresponding to case 8, case 9, and case 10, respectively), the graph shows a consistent increase in heat transfer with higher nanoparticle percentage. The fact that instance 10 achieves the greatest "heat transfer rate of 76.73 W" suggests that TiO_2 nanoparticles function best at greater concentrations. The output coolant temperature also drops with increasing TiO_2 nanoparticle concentration; case 10 has the lowest outlet temperature. This result demonstrates the TiO_2 nanoparticles' higher thermal performance, where heat removal from the coolant is most successfully achieved via the accelerated heat transfer mechanism.

Overall, the use of nanoparticles improves heat transfer in the flat tube radiator, with TiO_2 nanoparticles demonstrating the best performance due to their ability to sustain high heat transfer rates and lower the coolant outlet temperature effectively.

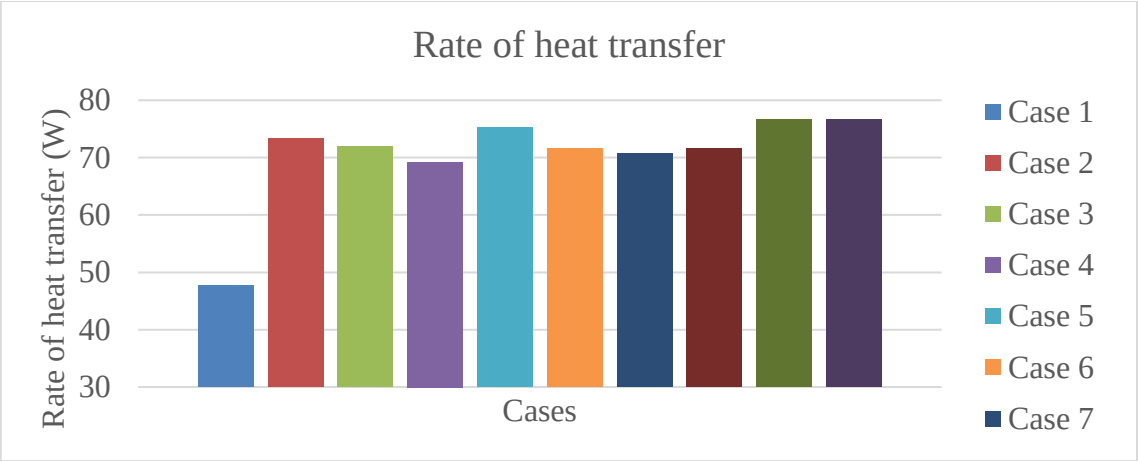

Figure 16 Rate of heat transfer graph representation for all case

V. CONCLUSION

Improving the cooling capability of car engines is the main goal of improving heat transmission across the coolant and radiator, guaranteeing peak performance and averting malfunctions. This study explores two methods for achieving this goal. The first involves modifying the radiator’s flat tube design by altering the fin configuration. One design features 34 continuous louvered fins, while the other includes 46 continuous louvered fins with a U-shaped configuration. In order to improve heat transmission, the second technique adds solid particles that are nanoscale to the base fluid. At 0.05%, 0.15%, and 0.3% concentrations, three nanoparticles— Al_2O_3, CuO, and TiO_2—are used. By combining the modified designs with these nanoparticles at varying concentrations, a total of 10 cases were analyzed. In order to improve the heat transfer in flat tube, the study's findings demonstrate how well these techniques work to enhance heat transfer performance.

- Heat transfer is directly proportional to area that absorb heat.

- Addition of fins in the flat tube occur the increment is the heat transfer resultant decreases in the outlet temperature of coolant.
- In terms of adding the nanoparticle is give the enhancement in heat transfer between the coolant and tube.
- In terms of Al_2O_3 nanoparticle, increasing in concentration, decreases the outlet coolant temperature. Lowest outlet temperature of 361.838 K achieve in case 4 which correspond to 0.3% concertation of Al_2O_3.
- In terms of CuO nanoparticle, increases in concentration, increases the outlet temperature of coolant. Lowest outlet temperature of 361.755 K achieve in case 5 which correspond to 0.05% concentration of CuO.
- In terms if TiO_2 nanoparticle, increases in concentration, decreases the outlet temperature of coolant. Lowest outlet temperature of 360.53 K achieve in case 10 which correspond to 0.3% concentration of TiO_2.
- Among the all cases, lowest outlet temperature, of 360.53 K and highest rate of heat transfer 76.73 W is in case 10, which is correspond to TiO_2 nanoparticle with 0.3% concentration.
- From the study of enhancement of heat transfer by addition of nanoparticle with distinct concentration case 10 having TiO_2 nanoparticle at 0.3% concentration shows better result as compare to all cases.

VI. REFERENCES

[1] V. R. Patil, S. S. Patil, and V. Kumbhar, "Review of Problems of Heat Transfer in Car Radiator and Suggested Solutions," *Int. J. Sci. Dev. Res.*, vol. 2, no. 1, pp. 94–98, 2017, [Online]. Available: http://www.ijsdr.org/papers/IJSDR1701016.pdf

[2] I. N. Ibrahim, N. Sazali, A. S. Jamaludin, D. Ramasamy, S. M. Soffie, and M. H. D. Othman, "A review on vehicle radiator using various coolants," *J. Adv. Res. Fluid Mech. Therm. Sci.*, vol. 59, no. 2, pp. 330–337, 2019.

[3] R. Kumar, D. Yadav, A. Verma, and Dr.G.R.Selokar, "A REVIEW ON EXPERIMENTAL INVESTIGATION AND TEMPERATURE DISTRIBUTION OF AUTOMOBILE RADIATOR USING NANO FLUIDS," no. 6, pp. 1596–1602, 2019.

[4] V. Amrit and G. Dude, "Investigation of cooling performance of automobile radiator with water based TiO 2 nano-fluid," vol. 6, no. 4, pp. 181–185, 2019, [Online]. Available: www.jetir.org

[5] A. Liu, G. Wang, D. Wang, X. Peng, and H. Yuan, "Study on the thermal and hydraulic performance of fin-and-tube heat exchanger based on topology optimization," *Appl. Therm. Eng.*, vol. 197, no. March, p. 117380, 2021, doi: 10.1016/j.applthermaleng.2021.117380.

[6] T. K. Ibrahim, A. T. Al-Sammarraie, M. S. M. Al-Jethelah, W. H. Al-Doori, M. R. Salimpour, and H. Tao, "The impact of square shape perforations on the enhanced heat transfer from fins: Experimental and numerical study," *Int. J. Therm. Sci.*, vol. 149, no. October 2019, p. 106144, 2020, doi: 10.1016/j.ijthermalsci.2019.106144.

[7] K. Kumar and A. Agrawal, "'Optimizing Heat Transfer Efficiency with Nanofluids in Automotive Radiator Applications for Enhanced Performance: A Comprehensive Review Article of Research Findings,'" *Int. J. Res. Appl. Sci. Eng. Technol.*, vol. 11, no. 10, pp. 1189–1194, 2023, doi: 10.22214/ijraset.2023.56164.

[8] K. David and A. Kumar, "CFD and Heat Transfer Analysis ofAutomobile Radiator Using Helical Tubes," *Int. J. Innov. Res. Sci. Eng. Technol.*, vol. 8, no. 5, pp. 5988–6017, 2019, doi: 10.15680/IJIRSET.2019.0805138.

[9] Mukesh Kumar Singh, "A Review on Internal Combustion Engine Fins," *Int. J. Eng. Res.*, vol. V9, no. 08, pp. 802–804, 2020, doi: 10.17577/ijertv9is080311.

[10] F. B. Majmader and M. J. Hasan, "Thermal enhancement and entropy generation of an air-cooled 3D radiator with modified fin geometry and perforation: A numerical study," *Case Stud. Therm. Eng.*, vol. 52, no. October, p. 103671, 2023, doi: 10.1016/j.csite.2023.103671.

[11] R. Kirubagharan, C. Ramesh, P. Pragalathan, and N. Harish, "Geometrical analysis of automobile radiator using CFD," *Mater. Today Proc.*, vol. 33, no. xxxx, pp. 3124–3130, 2020, doi: 10.1016/j.matpr.2020.03.739.

[12] M. Rama, M. Anil Kumar, A. T. Vemunuri, and N. Teja Valusa, "Design and Thermal Analysis of an Automotive Radiator for enhancing Flow Uniformity using CFD," *Int. Res. J. Eng. Technol.*, pp. 2872–2879, 2022, [Online]. Available: www.irjet.net

[13] S. Mert, H. Yasar, U. Durmaz, A. Topuz, A. Yeter, and T. Engin, "AN EXPERIMENTAL STUDY ON COOLING PERFORMANCE OF A CAR RADIATOR USING Al2O3-ETHYLENE

GLYCOL/WATER NANOFLUID," *Therm. Sci.*, vol. 25, no. 1 Part B, pp. 801–809, 2021, doi: 10.2298/TSCI190630179M.

[14] J. Liu, S. Hussain, W. Wang, G. Xie, and B. Sundén, "Experimental and numerical investigations of heat transfer and fluid flow in a rectangular channel with perforated ribs," *Int. Commun. Heat Mass Transf.*, vol. 121, no. December 2020, 2021, doi: 10.1016/j.icheatmasstransfer.2020.105083.

[15] D. Kumar and G. S. Sokhal, "Numerical analysis of performance of water-based nanofluid flowing through tube bent at 90°," *Heat Transf. - Asian Res.*, vol. 49, no. 1, pp. 18–32, 2020, doi: 10.1002/htj.21597.

[16] N. Tran and C. C. Wang, "Optimization of the airside thermal performance of mini-channel-flat-tube radiators by using composite straight-and-louvered fins," *Int. J. Heat Mass Transf.*, vol. 160, p. 120163, 2020, doi: 10.1016/j.ijheatmasstransfer.2020.120163.

[17] P. Sharma, V. Kumar, G. S. Sokhal, G. Dasaroju, and V. K. Bulasara, "Numerical study on performance of flat tube with water based copper oxide nanofluids," *Mater. Today Proc.*, vol. 21, pp. 1800–1808, 2020, doi: 10.1016/j.matpr.2020.01.234.

[18] N. Arora and M. Gupta, "An updated review on application of nanofluids in flat tubes radiators for improving cooling performance," *Renew. Sustain. Energy Rev.*, vol. 134, no. August, p. 110242, 2020, doi: 10.1016/j.rser.2020.110242.

[19] P. Abhilash, U. Raghupathi, and P. Kumar, "Design and testing of radiator with fixed channel and helical pipe using nanofluids," *Mater. Today Proc.*, vol. 39, no. xxxx, pp. 615–620, 2020, doi: 10.1016/j.matpr.2020.09.002.

[20] A. S. Tijani and A. S. bin Sudirman, "Thermos-physical properties and heat transfer characteristics of water/anti-freezing and Al2O3/CuO based nanofluid as a coolant for car radiator," *Int. J. Heat Mass Transf.*, vol. 118, pp. 48–57, 2018, doi: 10.1016/j.ijheatmasstransfer.2017.10.083.

[21] A. A. Permanasari, B. S. Kuncara, P. Puspitasari, S. Sukarni, T. L. Ginta, and W. Irdianto, "Convective heat transfer characteristics of TiO2-EG nanofluid as coolant fluid in heat exchanger," *AIP Conf. Proc.*, vol. 2120, no. July, 2019, doi: 10.1063/1.5115691